Desalination and Water Treatment
www.deswater.com

doi: 10.1080/19443994.2015.1088476

57 (2016) 17826–17835
August

Taylor & Francis
Taylor & Francis Group

Kinetic, isotherm and thermodynamic studies for the removal of Pb^{2+} ion by a novel adsorbent *Luffa acutangula* (LAPR)

Rais Ahmad*, Shaziya Haseeb

Environmental Research Laboratory, Faculty of Engineering and Technology, Department of Applied Chemistry, Aligarh Muslim University, Aligarh 202002, UP, India, Tel. +91 0571 2700920 23, ext. 3000; Fax: +91 0571 2400528; emails: rais45@rediffmal.com (R. Ahmad), Shaziya.shoaib@gmail.com (S. Haseeb)

Received 24 February 2015; Accepted 22 August 2015

ABSTRACT

Luffa acutangula peel (LAP) is a cheap material easily available in northern regions of India. LAP in the raw (LAPR) form shows excellent adsorption efficiency towards Pb^{2+} (98%). The effect of various contact time, concentration, pH, and temperature was studied and it was found that reaction is endothermic and spontaneous in nature. Maximum adsorption was observed at 120 min at pH 6. Kinetic study was best obeyed by pseudo-second order. The equilibrium data were best fitted by D–R isotherm. The functional and morphological properties of adsorbents were characterized by FTIR, SEM, and EDX techniques.

Keywords: Adsorption; D–R (Dubinin–Radushkevich); SEM; EDX; Endothermic; LAPR

1. Introduction

In recent decades, earth's population has grown exponentially and demands for durable and non-durable goods have followed the same trend, resulting in industrial growth to meet human needs. As a result of this industrialization, the environmental impact of effluents containing toxic substances is becoming increasingly apparent. Heavy metals are still being used in various industries due to their technological importance. Yet, imperfect treatment of waste products from these industries may lead to both human health and environmental issues [1]. Considering the harmful effects of heavy metals, it becomes then necessary to remove them from liquid wastes at least to the limit accepted by the regulations. Pb^{2+} ion is one of the hazardous metals used in various industries like electroplating, mining and battery manufacturing, etc. Lead, a dominant poisonous metal, is one of the most hazardous elements to human health, even in low concentrations [2]. It can damage nervous connections, and cause blood and brain disorders [3]. Lead poisoning typically results from consuming contaminated food or water, but it can also occur after accidental ingestion of contaminated soil, dust, or lead-based paints [4]. Long-term exposure to lead or its salts, especially soluble salts or the strong oxidant PbO_2, can cause nephropathy and colic-like abdominal pains [5]. Therefore, it's a long time that the extraction and determination of lead ions in food samples has been a subject of interest worldwide. Among various purification technologies, biosorption has been considered as one of the most efficient and environmentally friendly technology to remove heavy metals from wastewater systems [6,7].

*Corresponding author.

In recent years, biosorbents have been considered as the cheapest, most abundant, and environment-friendly options and a vast number of literatures have been devoted to the removal of heavy metals from wastewater by using adsorption technique with different low cost materials [7–9]. Most of the adsorption studies use waste plant material such as xanthum gum [10], cashew nut [11], walnut wood activated carbon [12], and iron powder activated carbon [13] because they require simple technique, easy processing, good adsorption capacity, free availability, and easy regeneration.

Luffa acutangula or simply called ridged gourd or Turai (in Hindi) is a cheap vegetable easily available in India. This vegetable is a rich source of fat, carbohydrate, potassium. This adsorbent is a novel adsorbent for the removal of Pb^{2+}. This adsorbent can remove up to 98% of Pb^{2+} from aqueous solution. In this study, peels of *L. acutangula* were used in the raw form for the removal of Pb^{2+}. The effect of various parameters such as equilibrium time, pH, and temperature was also studied. The characterization of the adsorbent was also carried out to study the functional and morphological properties of the adsorbent.

2. Materials and methods

2.1. Materials and instruments

All the chemicals were of analytical grade. Stock solutions (1,000 mg L^{-1}) of metal nitrate salts were prepared in double distilled water.

The photomicrography of the exterior surface of adsorbent was obtained by scanning electron microscopy (JSM-6510LV). The functional groups were characterized by FTIR model (Perkin Elmer, USA, model spectrum-BX, range 4,000–400 cm^{-1}). The elemental characteristics were obtained by the EDX model (JSM-6510LV). The adsorption characteristics were determined by atomic absorption spectroscopy (AAS) model (GBC-902, Australia). The pH was measured by pH meter (Elico L1 120, India).

2.2. Adsorbent preparation

The *L. acutangula* peel (LAP) was collected as a waste from local market. It was washed with distilled water and then converted into micro particles by grinding them in a mechanical grinder followed by sieving of mesh size 50–100. It was then, again washed several times with double distilled water to remove dirt, color, and impurities. Further, it was dried and used for the adsorption studies.

2.3. Batch adsorption experiments

2.3.1. Metal selectivity test

The selective nature of LAPR was studied for Pb^{2+}, Cu^{2+}, Ni^{2+}, and Cd^{2+}. It follows as $Pb^{2+} > Cu^{2+} > Ni^{2+} > Cd^{2+}$.

2.3.2. Adsorption study

Adsorption studies were carried out in batch process. Solutions of metals Pb^{2+} (50 mL) of desired concentrations (10–100 mg L^{-1}) were equilibrated with 0.1 g of adsorbent (LAPR) in 250-mL conical glass flask. The mixtures were kept at room temperature for 24 h. After equilibration, the samples were filtered and taken for AAS analysis. The samples were analyzed in triplicates and adsorption capacity values at equilibrium (q_e) were calculated using the following relationship:

$$q_e = \frac{(C_o - C_e)V}{W} \quad (1)$$

where q_e is the adsorption capacity at equilibrium, C_o is the initial concentration of the adsorbate (mg L^{-1}) and C_e is the concentration of adsorbate at equilibrium (mg L^{-1}), V is the volume of the solution (L) and W is the mass of the adsorbent (g).

The influence of pH was studied in the pH range 2–8. The pH was adjusted using 0.5 M HCl and 0.5 M NaOH. The batch experiment was carried out using 0.1 g of adsorbents and 50 mL of 50 mg L^{-1} metal ion solution. The effect of electrolyte on pH was also studied.

2.3.3. Point of zero charge

Solid addition method [14] was used to determine the zero surface charge characteristics (pH_{zpc}) of LAPR using 0.1 M KCl solution. The total volume of the solution was adjusted exactly to 25 mL in a conical flask by adding 0.1 M KCl. The initial pH (pH_i) of the solutions was adjusted between 2 and 10 by adding 0.5 M HCl and 0.5 M NaOH solutions. The pH_i of the solutions was then accurately noted and 0.1 g of adsorbent was added to the series of different pH_i solutions and the suspension was allowed to equilibrate for 24 h. The final pH (pH_f) of the supernatant liquid was noted. The difference between the initial pH (pH_i) and final pH (pH_f) values ($\Delta pH = pH_i - pH_f$) was plotted against pH_i. The point of intersection of the resulting curve with the abscissa, at which $\Delta pH = 0$, gave the pH_{zpc} value.

3. Results and discussions

3.1. Characterization of the LAPR

The SEM micrograph for LAPR before and after adsorption is shown in Fig. 1(a) and (b). The SEM micrograph shows the adsorbent is porous in nature. After metal loading there is a distinct change in the surface morphology. The FTIR spectra for the Pb^{2+} adsorption before and after adsorption are shown in Fig. 2. The peaks at 2,924.57 cm^{-1} correspond to C–H stretching vibrations of the methyl groups present on the surface of the adsorbent [15]. The peak at 1,642.57 cm^{-1} corresponds to C=C bonds. The peaks at 1,032.35 cm^{-1} correspond to lignin structure. The shift from 1,427.60 to 1,425.36 cm^{-1} corresponds to the presence of carbonate groups and adsorption of Pb^{2+} ions onto *L. acutangula*. The peaks at 3,410 cm^{-1} correspond to the presence of carboxylic groups. The peaks at 668.42 cm^{-1} correspond to –C–H bonds. Among the functional groups, hydroxyl, amines and carboxyl group bind heavy metal ion with the adsorbent [16]. The results of EDX before and after adsorption show the presence of elements with weight % composition in LAPR as carbon (57.47%), oxygen (42.53%), and lead (0.39%) as shown in Fig. 3(a) and (b).

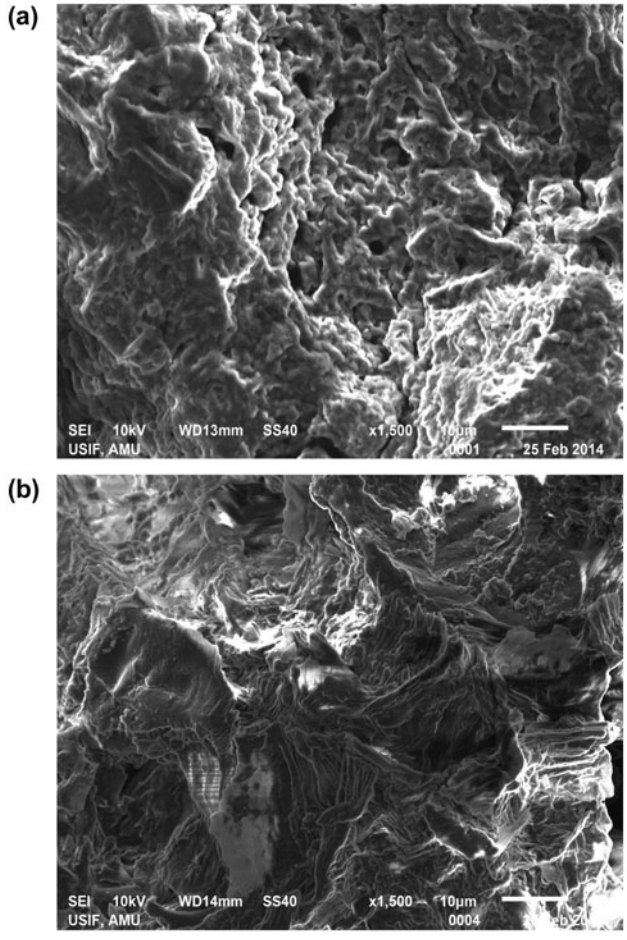

Fig. 1. SEM micrograph of LAPR (a) before adsorption and (b) after adsorption of Pb^{2+} ion.

3.2. Effect of operating parameters

The contact time for the adsorbents (LAPR) was studied in the range of 5–180 min at 25℃ for 10, 50, and 100 mg L^{-1} as shown in Fig. 4. It was found that maximum adsorption was attained in 120 min for Pb^{2+} ion. The rapid uptake of metal ion on the adsorbent may indicate that most of the reaction sites of the adsorbent were exposed for interaction with metal ion. Furthermore, the presence of hydroxyl group in adsorbent forms a complex between metal ion and adsorbent surface causing faster adsorption.

The pH plays an important role in the adsorption of metal ions. The effect of pH for LAPR on Pb^{2+} is shown in Fig. 5. The maximum adsorption for the LAPR is obtained at pH 6. After pH 6, the solution tends to precipitate due to formation of hydroxide ion [17–19]. At lower pH values, H_3O^+ ions compete with metal ions for exchange and therefore the Pb^{2+} ion uptake decreased at lower pH. The competitive adsorption occurred between H^+ protons and free metal ions and their hydroxide fixation sites [20]. The point of zero charge for LAPR was observed at pH 5.0 which is lower than the equilibrium pH of the Pb^{2+} ion which shows adsorbent surface is positively charged due to protonation as shown in Fig. 6.

3.3. Adsorption kinetics

In order to examine the controlling mechanism of adsorption process such as mass transfer and chemical reaction, pseudo-first order, pseudo-second order, intraparticle diffusion and Elovich equation were used to test the experimental data.

The pseudo-first-order reaction equation of Lagergren [21] was widely used for the adsorption of liquid/solid system on the basis of solid capacity. The linearized form of equation is as follows:

$$\log(q_e - q_t) = \log q_e - \frac{k_1 t}{2.303} \quad (2)$$

where q_e is the adsorption capacity at equilibrium (mg g^{-1}), q_t is the adsorption capacity at time t (mg g^{-1}), and k_1 is the rate constant (min^{-1}). k_1 and R^2 of Pb^{2+} under different concentrations were calculated

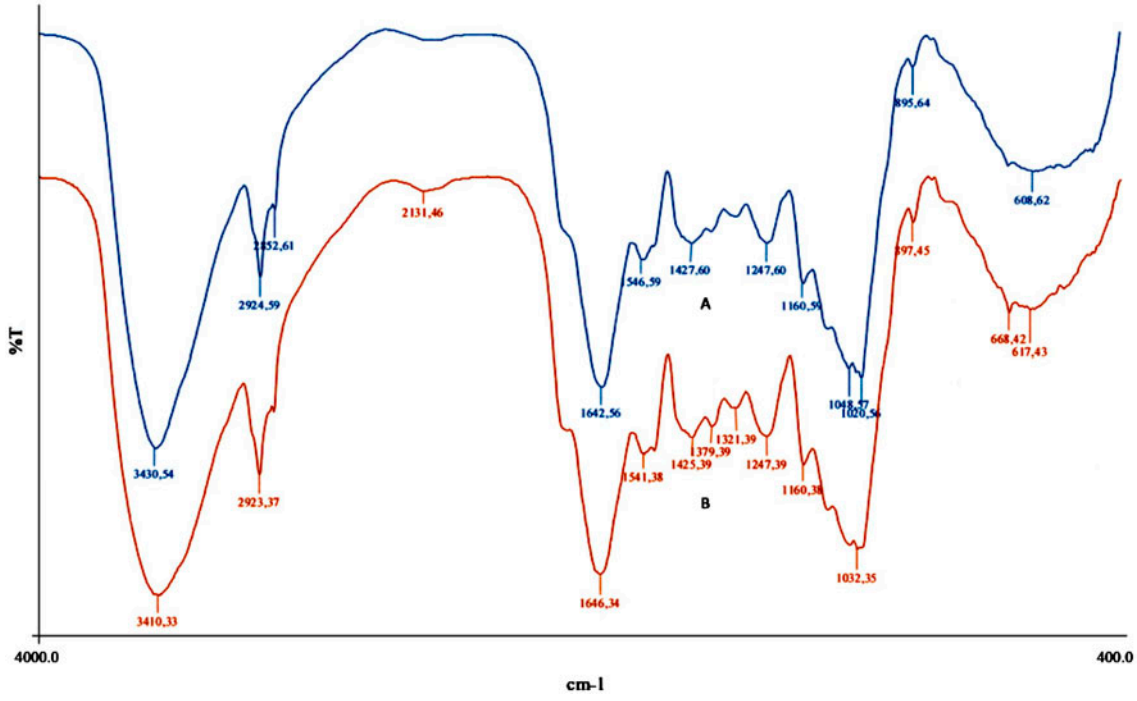

Fig. 2. FTIR spectra of LAPR for the Pb^{2+} adsorption (a) before adsorption and (b) after adsorption.

from the linear plot of $\log(q_e - q_t)$ vs. t as shown in Fig. 7 and Table 1. The calculated values of q_e do not match with the experimental values of q_e and R^2 values are also low; so, it does not follow pseudo-first-order kinetics.

Pseudo-second-order rate equation was expressed as:

$$\frac{t}{q_t} = \frac{1}{k_2 q_e^2} + \frac{t}{q_e} \tag{3}$$

where k_2 is the pseudo-second-order rate constant (g mg min^{-1}). Plots of t/q_t vs. t for all experimental concentrations gave a straight line as shown in Fig. 8 and the values of q_e and k_2 were calculated from the slope and intercept, respectively. The value of q_e calculated was found to be close to q_e experimental, $q_{e\,(exp)}$. The values of correlation coefficient (R^2) were also found to be very close to 1, therefore it can be concluded that pseudo-second-order model was best fitted with the experimental data.

The intraparticle diffusion model [22] was expressed as:

$$q_t = K_{id} t^{1/2} + C \tag{4}$$

where K_{id} (mg g^{-1} $min^{-1/2}$) is the intraparticle diffusion constant and q_t is the adsorption capacity at time t (mg g^{-1}). The value of K_{id}, C, and R^2 were calculated from the slope of plot q_t vs. $t^{1/2}$ as shown in Fig. 9 and given in Table 1. The value of intercept gives an idea about the boundary layer thickness i.e. larger the intercept; greater is the boundary layer effect. It is seen from Table 1, the value of intercept is not zero but high and it increases with increase in concentration of the metal ion as compared to mass film control diffusion. This result implies that boundary layer diffusion is the rate controlling step.

The Elovich equation is expressed as follows:

$$q_t = A + B \ln t \tag{5}$$

where A nd B are the constants as shown in Table 1. The Elovich equation is used to describe the sorption system if it is chemisorption [23]. The R^2 values are low and therefore it does not follow this model.

3.4. Adsorption isotherms

Adsorption isotherms are important parameters to study the interaction of molecules or ions with the adsorbent sites and the degree of accumulation. In this study, various isotherm models were studied like Langmuir, Freundlich, Temkin, D–R (Dubinin–Radushkevich) isotherm, and Halsey isotherm for the Pb^{2+} ion.

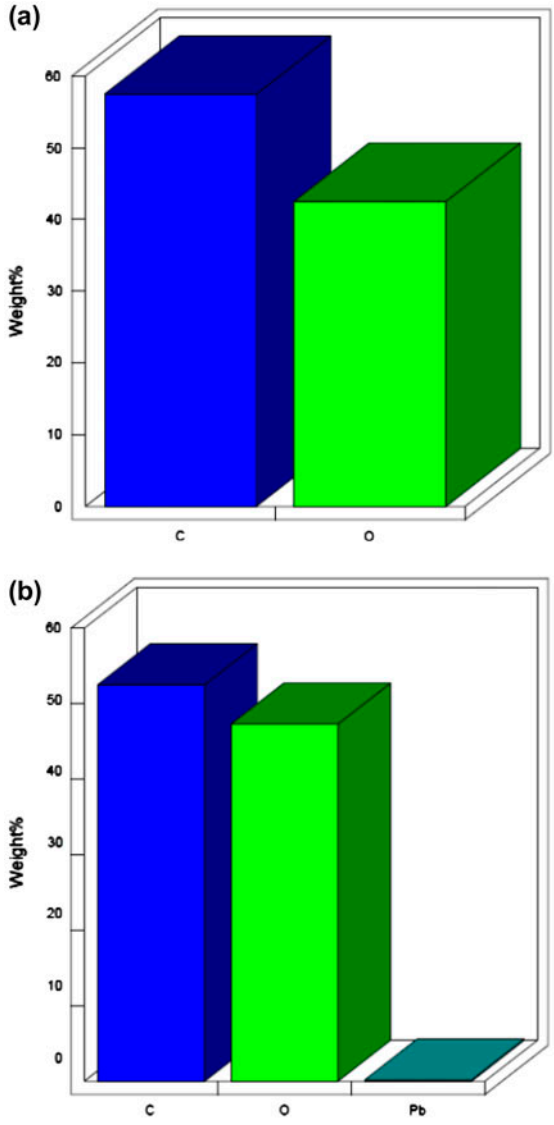

Fig. 3. EDX graph of LAPR (a) before adsorption and (b) after adsorption of Pb^{2+} ion.

Langmuir isotherm model is given as:

$$\frac{1}{q_e} = \frac{1}{bq_m} + \frac{1}{q_m}\frac{1}{C_e} \quad (6)$$

Freundlich isotherm model is given as:

$$\log q_e = \log K_F + \frac{1}{n} \log C_e \quad (7)$$

Temkin isotherm model is given as:

$$q_e = B_1 \ln K_T + B_1 \ln C_e \quad (8)$$

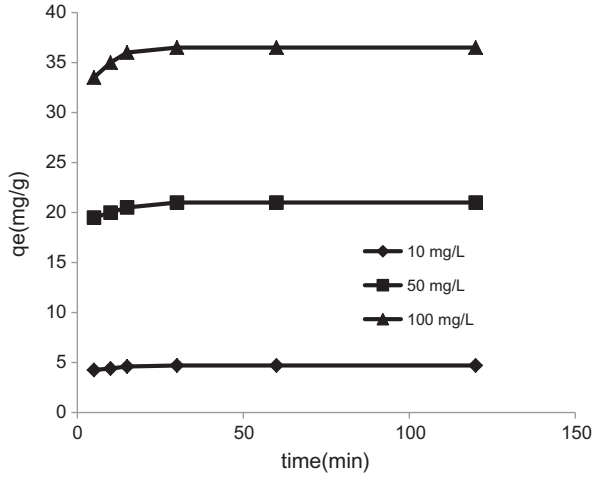

Fig. 4. Effect of contact time for the adsorption of Pb^{2+} ion on LAPR.

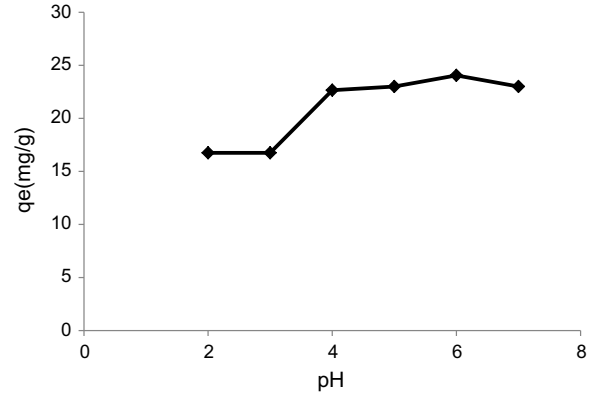

Fig. 5. Effect of pH for the adsorption of Pb^{2+} ion on LAPR.

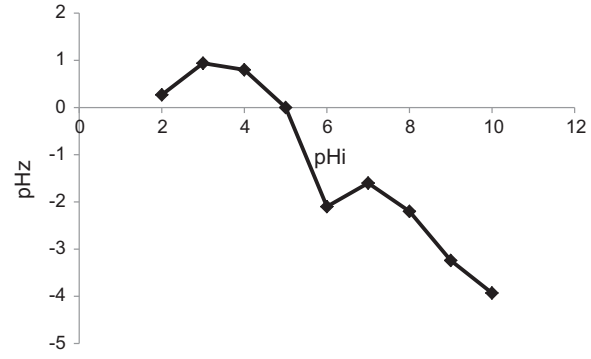

Fig. 6. Point of zero charge of the adsorbent (LAPR).

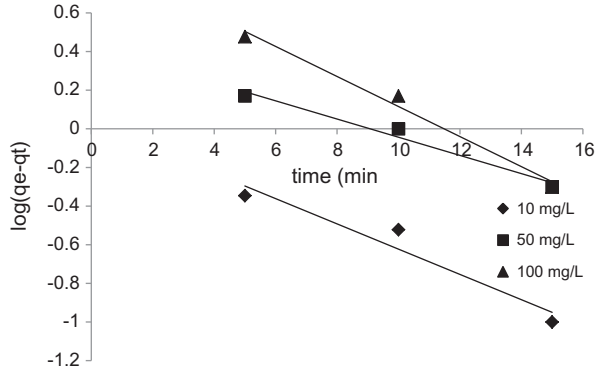

Fig. 7. Pseudo-first-order for the adsorption of Pb^{2+} ion on LAPR.

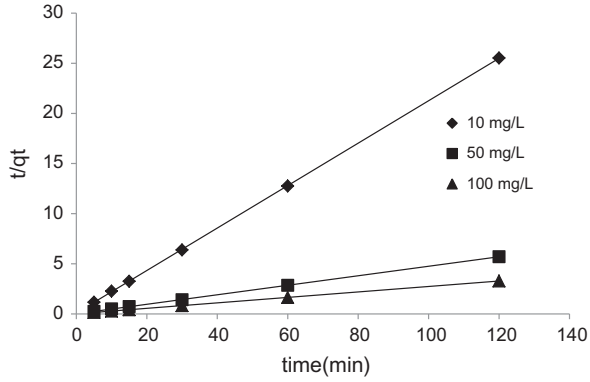

Fig. 8. Pseudo-second-order for the adsorption of Pb^{2+} ion on LAPR.

Table 1
Kinetic parameters for the adsorption of Pb^{2+} ion onto LAPR

S. no.	Parameters	10 mg L^{-1}	50 mg L^{-1}	100 mg L^{-1}
(1)	*Pseudo-first-order*			
	$Q_{e(cal)}$	1.07	2.67	7.81
	$Q_{e(exp)}$	4.7	21	36.5
	R^2	0.933	0.974	0.9854
	k_1	0.149	0.1084	0.1773
(2)	*Pseudo-second-order*			
	$Q_{e(cal)}$	4.7	21	36.5
	$Q_{e(exp)}$	4.7	21	36.5
	R^2	1	1	1
	k_2	2.39×10^{-2}	3.29×10^{-4}	16.33×10^{-4}
(3)	*Intraparticle diffusion*			
	K_{id}	0.142	0.469	0.911
	C	3.96	18.52	31.89
	R^2	0.922	0.973	0.872
(4)	*Elovich equation*			
	A	4.1069	18.962	32.883
	B	0.1433	0.4884	0.8853
	R^2	0.7809	0.8256	0.737

Dubinin–Radushkevich isotherm model is given as:

$$\ln q_e = \ln q_m - \beta \in^2 \quad (9)$$

Halsey isotherm model is given as:

$$\ln q_e = \left[\left(\frac{1}{n_H}\right) \ln K_H - \left(\frac{1}{n_H}\right)\frac{1}{C_e}\right] \quad (10)$$

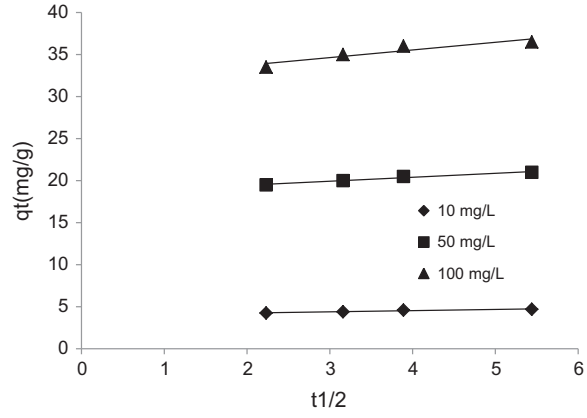

Fig. 9. Intraparticle diffusion for the adsorption of Pb^{2+} ion on LAPR.

The Langmuir adsorption isotherm model was applied for the determination of maximum adsorption capacity corresponding to complete monolayer coverage onto the adsorption surface of a finite number of the identical sites. The Freundlich isotherm is based on an empirical equation where the adsorption took place on the heterogeneous surface of the adsorbent.

The Freundlich isotherm constants n and K_F are empirical parameters that vary with the degree of heterogeneity and are related to adsorption capacity. The values of n should lie between 1 and 10 for the favorable adsorption process. Halsey isotherm model was used to explain the multilayer adsorption system for Pb^{2+} ions. Temkin isotherm model was applied to evaluate the adsorption potentials of adsorbents for adsorbates, i.e. Pb^{2+} ions from aqueous solution. Harkins–Jura isotherm model suggested the multilayer adsorption as well as heterogeneous pore distribution in the adsorbents surface [19]. All the isotherm

parameters along with correlation coefficient (R^2) are shown in Table 2. The plots of various isotherms for LAPR are shown in Figs. 10–13. The sorption energy was calculated using Dubinin–Radushkevich isotherm [24] to predict the nature of adsorption process i.e. physical or chemical.

The value obtained from the plots predicts that LAPR is best followed by D–R isotherm as shown in Table 2. The higher regression coefficient value and high value of q_m show that LAPR was best fitted by D–R Isotherm. The value of apparent energy also shows the process is physiosorption and its heterogeneous nature shows that the adsorbent was best fitted by Dubinin–Radushkevich (D–R) isotherm [25].

3.5. Thermodynamic studies

The thermodynamic factors were studied in the temperature range of 303–323 K. The thermodynamic parameters such as enthalpy change (ΔH°), entropy change (ΔS°) and Gibbs free energy change (ΔG°) were estimated using the following equation [26]:

$$K_c = \frac{C_s}{C_e} \tag{11}$$

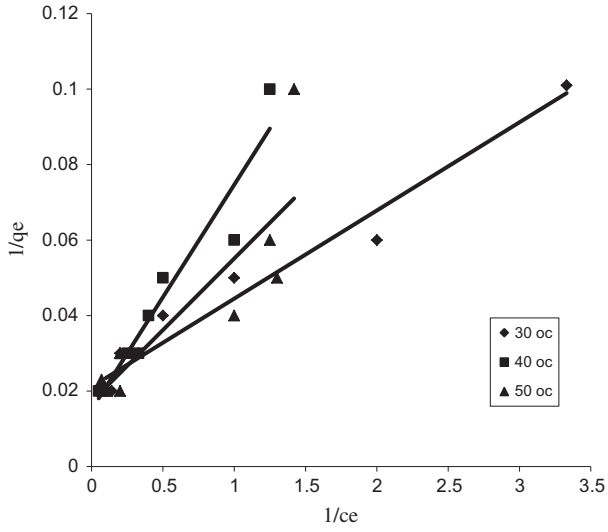

Fig. 10. Langmuir isotherm for the adsorption of Pb^{2+} ion on LAPR.

where K_c is the equilibrium constant, C_s the solid phase concentration at equilibrium (mg L^{-1}), C_e is the equilibrium concentration in solution (mg L^{-1}).

Table 2
Adsorption isotherm of LAPR for Pb^{2+} ion

S. no.	Parameters	30℃	40℃	50℃
(1)	*Langmuir isotherm*			
	Q_m	47.39	16.80	26.38
	b	10.001	3.941	2.203
	R^2	0.961	0.931	0.730
(2)	*Freundlich isotherm*			
	K_F	17.87	19.97	17.33
	$1/n$	0.401	0.241	0.376
	R^2	0.981	0.600	0.766
(3)	*Temkin isotherm*			
	B_1	9.459	6.003	9.111
	K_T	8.239	39.60	7.96
	R^2	0.962	0.962	0.864
(4)	*D–R isotherm*			
	β	0.1832	0.1688	0.1788
	Q_m	48.09	50.97	49.34
	R^2	0.949	0.909	0.929
	E	1.652	1.72	1.67
(5)	*Halsey isotherm*			
	$1/n_H$	0.4087	0.3815	0.3777
	K_H	0.111×10^{-3}	0.116×10^{-3}	0.188×10^{-3}
	R^2	0.984	0.834	0.781

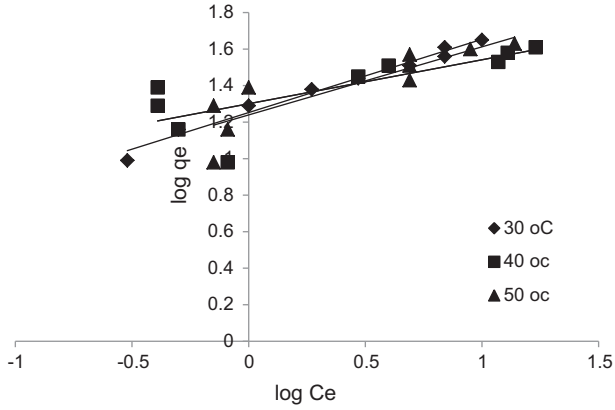

Fig. 11. Freundlich isotherm for the adsorption of Pb^{2+} ion on LAPR.

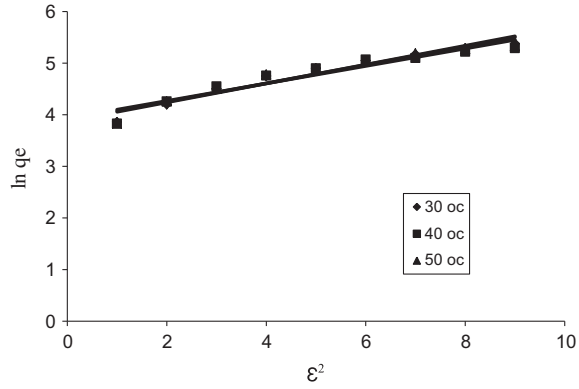

Fig. 13. D–R isotherm for the adsorption of Pb^{2+} ion on LAPR.

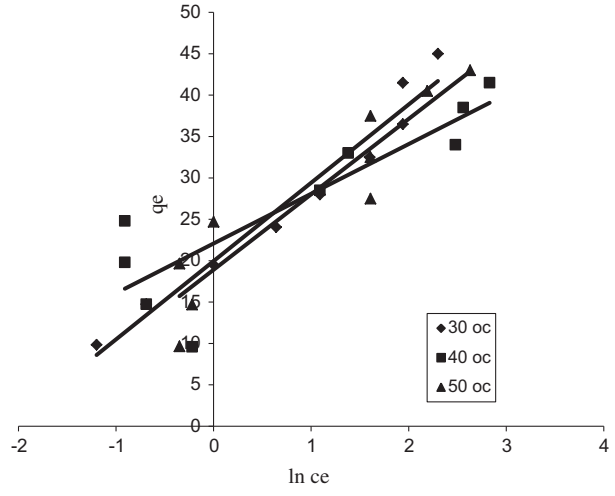

Fig. 12. Temkin isotherm for the adsorption of Pb^{2+} ion on LAPR.

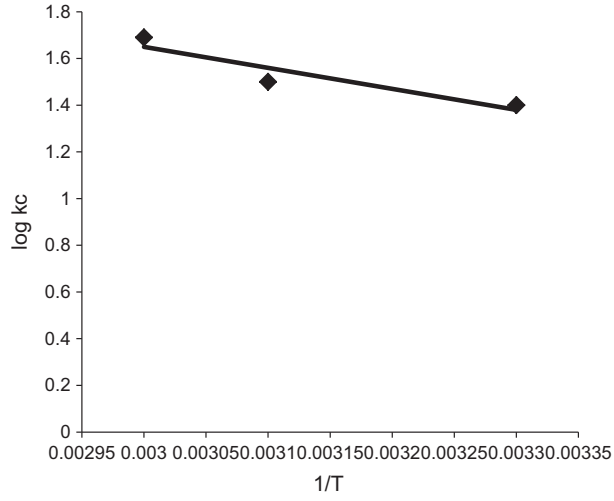

Fig. 14. Plot of log K_c vs. $1/T$ for the adsorption of Pb^{2+} ion.

Table 3
Thermodynamic parameters for the adsorption of Pb^{2+} ion

Temp. (K)	$1/T$	ln K_c	log K_c	ΔG° (kJ mol^{-1} K^{-1})	ΔH° (kJ mol^{-1} K^{-1})	ΔS° (kJ mol^{-1})	R^2
303	0.0033	3.23	1.40	−8.13	17.23	0.083	0.871
313	0.0031	3.47	1.50	−9.02			
323	0.003	3.89	1.69	−10.4			

$$\Delta G^\circ = -RT \ln K_c \quad (12)$$

$$\log K_c = \frac{\Delta S^\circ}{2.303R} - \frac{\Delta H^\circ}{2.303RT} \quad (13)$$

ΔH° and ΔS° were determined by Van't Hoff equation.

The values of ΔH° and ΔS° were obtained from the slope and the intercept of the plot log K_c vs. $1/T$ as shown in Fig. 14 and presented in Table 3. The values of ΔG° are negative confirming the adsorption of Pb^{2+} ion onto LAPR is spontaneous and thermodynamically favorable at high temperature. The positive value of ΔH° and ΔS° indicate the endothermic nature and the randomness at solid/liquid solution interface during the adsorption of Pb^{2+} ion on LAPR, respectively.

Table 4
Comparison of the uptake capacities for copper(II) ions of various adsorbents

Adsorbent	Q_{max} (mg g^{-1})	Refs.
Commercial activated carbon	5.90	[27]
Almond shell	8.08	[28]
Kaolinite	7.75	[29]
Chitosan immobilized on bentonite	15.00	[30]
Cocoa pod husk	20.10	[31]
Barley straws	23.20	[32]
Mushrooms	27.10	[33]
Olive tree pruning waste	27.40	[34]
Hazelnut shell	28.20	[28]
Luffa acutangula peels	47.39	[Present study]

3.6. Comparative study of the adsorbent

In order to evaluate the feasibility of the adsorbent and to compare the adsorption capacity with other non-conventional adsorbents, a comparative study is presented in Table 4. It is evident from the table that LAPR has got the highest monolayer adsorption capacity (47.39 mg g^{-1}) among all the adsorbents.

4. Conclusions

In this work, *L. acutangula* peels (LAPR) have been proved to be a very good adsorbent for Pb^{2+} removal with a maximum adsorption of 98%. The maximum adsorption capacity of 24 mg g^{-1} is observed at optimum conditions of 120 min equilibrium time, pH 6.0, and temperature 25°C. The equilibrium data are best followed by pseudo-second-order kinetic model. The higher regression coefficient values show that LAPR is best fitted by D–R (Dubinin–Radushkevich) isotherm showing the heterogeneous and physiosorption process. The positive value of ΔH° and ΔS° indicate the adsorption process on LAPR is endothermic and spontaneous in nature with randomness at solid–liquid solution interface. The present adsorbent exhibits a maximum adsorption capacity among all the adsorbents and therefore the material can be utilized for the removal of Pb^{2+} from wastewater economically.

Acknowledgment

The author thanks the UP-CST (Uttar Pradesh-council of science and technology), Uttar Pradesh, India as funding agency for the financial support under the project no: D/352.

References

[1] J. Febrianto, A.N. Kosasih, J. Sunarso, Y.H. Ju, N. Indraswati, S. Ismadji, Equilibrium and kinetic studies in adsorption of heavy metals using biosorbent: A summary of recent studies, J. Hazard. Mater. 162 (2009) 616–645.
[2] A. Bahrami, A.B. Besharati-Seidani, A. Abbaspour, M. Shamsipur, A highly selective voltammetric sensor for sub-nanomolar detection of lead ions using a carbon paste electrode impregnated with novel ion imprinted polymeric nanobeads, Electrochim. Acta 118 (2014) 92–99.
[3] H. Ebrahimzadeh, A.A. Asgharinezhad, E. Moazzen, M.M. Amini, O. Sadeghi, A magnetic ion-imprinted polymer for lead(II) determination: A study on the adsorption of lead(II) by beverages, J. Food Compos. Anal. 41 (2015) 74–80.
[4] J.A. Ryan, K.G. Scheckel, W.R. Berti, S.L. Brown, S.W. Casteel, R.L. Chaney, J. Hallfrisch, M. Doolan, P. Grevatt, M. Maddaloni, D. Mosby, Reducing children's risk from lead in soil, Environ. Sci. Technol. 38 (2014) 18 A–24 A.
[5] A. Sabarudin, N. Lenghor, Y. Liping, Y. Furusho, S. Motomizu, Automated online preconcentration system for the determination of trace amounts of lead Using Pb-selective resin and inductively coupled plasma-atomic emission spectrometry, Spectrosc. Lett. 39 (2006) 669–682.
[6] A.H. Caravelli, L. Giannuzzi, N.E. Zaritzky, Reduction of hexavalent chromium by *Sphaerotilus natans* a filamentous micro-organism present in activated sludges, J. Hazard. Mater. 156 (2008) 214–222.
[7] M. Ghaedi, S. Hajati, F. Karimi, B. Barazesh, G. Ghezelbash, Equilibrium, kinetic and isotherm of some metal ion biosorption, J. Ind. Eng. Chem. 19 (2013) 987–992.
[8] D. Mohan, S. Rajput, V.K. Singh, D.H. Steele Jr., C.U. Pittman, Modeling and evaluation of chromium remediation from water using low cost bio-char, a green adsorbent, J. Hazard. Mater. 188 (2010) 319–333.

[9] R. Crisafully, M.A. Milhome, R.M. Cavalcante, Removal of some polycyclic aromatic hydrocarbons from petrochemical wastewater using low-cost adsorbents of natural origin, Bioresour. Technol. 99 (2008) 4515–4519.
[10] S. Ghorai, A.K. Sarkar, S. Pal, Rapid adsorptive removal of toxic Pb^{2+} ion from aqueous solution using recyclable, biodegradable nanocomposite derived from templated partially hydrolyzed xanthan gum and nanosilica, Bioresour. Technol. 170 (2014) 578–582.
[11] G.F. Coelho, A.C. Gonçalves Jr. Jr, C.R.T. Tarley, J. Casarin, H. Nacke, M.A. Francziskowski, Removal of metal ions Cd(II), Pb(II), and Cr(III) from water by the cashew nut shell *Anacardium occidentale* L., Ecol. Eng. 73 (2014) 514–525.
[12] M. Ghaedi, H. Mazaheri, S. Khodadoust, S. Hajati, M.K. Purkait, Application of central composite design for simultaneous removal of methylene blue and Pb^{2+} ions by walnut wood activated carbon, Spectrochim. Acta, Part A. 135 (2015) 479–490.
[13] L. Yuan, Y. Liu, Removal of Pb(II) and Zn(II) from aqueous solution by ceramisite prepared by sintering bentonite, iron powder and activated carbon, Chem. Eng. J. 215–216 (2013) 432–439.
[14] S. S Tripathy, S.B.Kanungo, Adsorption of Co^{2+}, Ni^{2+}, Cu^{2+} and Zn^{2+} from 0.5 M NaCl and major ion sea water on a mixture of δ-MnO_2 and amorphous FeOOH, J. Colloid Interface Sci. 284 (2005) 30–38.
[15] A. Kongsuwan, P. Patnukao, P. Pavasant, Binary component sorption of Cu(II) and Pb(II) with activated carbon from *Eucalyptus camaldulensis* Dehn bark, J. Ind. Eng. Chem. 15 (2009) 465–470.
[16] G. Bayramoğlu, M.Y. Yakup Arıca, Construction a hybrid biosorbent using *Scenedesmus quadricauda* and Ca-alginate for biosorption of Cu(II), Zn(II) and Ni(II): Kinetics and equilibrium studies, Bioresour. Technol. 100 (2009) 186–193.
[17] A. Özer, G. Gürbüz, A. Calimli, B.K. Körbahti, Biosorption of copper(II) ions on *Enteromorpha prolifera*: Application of response surface methodology (RSM), Chem. Eng. J. 146 (2009) 377–387.
[18] Y.P. Kumar, P. King, V.S.R.K. Prasad, Equilibrium and kinetic studies for the biosorption system of copper(II) ion from aqueous solution using *Tectona grandis* L.f. leaves powder, J. Hazard. Mater. 137 (2006) 1211–1217.
[19] A. Behmou coubi, A. Yaacoubi, L. Nibou, B. Tanouti, Adsorption of metal ions Moroccan stevensite*:* Kinetic and isotherm studies, J. Colloid Interface Sci. 282 (2005) 320–326.
[20] R. Ahmad, S. Haseeb, Adsorption of Cu^{2+} from aqueous solution onto agricultural solid waste-mentha: Characterization, isotherms, and kinetic studies, J. Dispersion Sci. Technol. 33 (2012) 1188–1196.
[21] S. Gupta, D. Kumar, J.P. Gaur, Kinetic and isotherm modeling of lead(II) sorption onto some waste plant materials, Chem. Eng. J. 148 (2009) 226–233.
[22] Y.S. Ho, G. McKay, Application of kinetic models to the sorption of copper(II) on to peat, Adsorpt. Sci. Technol. 20 (2002) 797–815.
[23] B. Singha, S. Das, Adsorptive removal of Cu(II) from aqueous solution and industrial effluent using natural/agricultural wastes, Colloids Surf., B 107 (2013) 97–106.
[24] M.A. Barakat, R. Kumar, Synthesis and characterization of porous magnetic silica composite for the removal of heavy metals from aqueous solution, J. Ind. Eng. Chem. 23 (2015) 93–99.
[25] J.C. Egwe, A.A. Abia, Equilibrium sorption isotherm studies of Cd(II), Pb(II) and Zn(II) ions detoxification from waste water using unmodified and EDTA-modified maize husk, Electron, J. Biotechnol. 10 (2007) 536–548.
[26] R. Ahmad, R. Kumar, Adsorption studies of hazardous malachite green onto treated ginger waste, J. Environ. Manage. 91 (2010) 1032–1038.
[27] A. Dubey, S. Shiwani, Adsorption of lead using a new green material obtained from Portulaca plant, Int. J. Environ. Sci. Technol. 9 (2012) 15–20.
[28] E. Pehlivan, T. Altun, S. Cetin, M.I. Iqbal Bhanger, Lead sorption by waste biomass of hazelnut and almond shell, J. Hazard. Mater. 167 (2009) 1203–1208.
[29] M.N. Sahmoune, K. Louhab, A. Boukhiar, Advanced biosorbents materials for removal of chromium from water and wastewaters, Environ. Prog. Sustain. Eng. 30 (2011) 284–293.
[30] C.M. Futalan, W.C. Tsai, S. Lin, K. Hsien, M.L. Dalida, M. Wan, Copper, nickel and lead adsorption from aqueous solution using chitosan-immobilized on bentonite in a ternary system, Sustain. Environ. Res. 22 (2012) 345–355.
[31] V.O. Njoku, A.A. Ayuk, E.E. Ejike, E.E. Oguzie, C.E. Duru, O.S. Bello, Cocoa pod husk as a low cost biosorbent for the removal of Pb(II) and Cu(II) from aqueous solutions, Aust. J. Basic Appl. Sci. 5 (2011) 101–110.
[32] E. Pehlivan, T. Altun, S. Parlayıcı, Utilization of barley straws as biosorbents for Cu^{2+} and Pb^{2+} ions, J. Hazard. Mater. 164 (2009) 982–986.
[33] R. Vimala, N. Das, Biosorption of cadmium(II) and lead (II) from aqueous solutions using mushrooms: A comparative study, J. Hazard. Mater. 168 (2009) 376–382.
[34] G. Blázquez, M.A. Martín-Lara, G. Tenorio, M. Calero, Batch biosorption of lead(II) from aqueous solutions by olive tree pruning waste: Equilibrium, kinetics and thermodynamic study, Chem. Eng. J. 168 (2011) 170–177.